

Open heavy-flavour production in pp and Pb–Pb collisions at the LHC, measured with ALICE at central rapidity

A Rossi for the ALICE Collaboration

Università di Padova and INFN - Sezione di Padova, Padova, Italy - now at CERN
email: andrea.rossi@cern.ch

August 15, 2019

Abstract

The ALICE experiment studies nucleus-nucleus collisions at the LHC in order to investigate the properties of QCD matter at extreme energy densities. The measurement of open charm and open beauty production allows to investigate the interaction of heavy quarks with the hot and dense medium formed in high-energy nucleus-nucleus collisions. In particular, in-medium energy loss is predicted to be different for gluons, light quarks and heavy quarks and to depend on the medium energy density and size. ALICE has measured open heavy-flavour particle production at central rapidity in several decay channels in Pb-Pb and pp collisions at $\sqrt{s_{NN}} = 2.76$ TeV and $\sqrt{s} = 2.76, 7$ TeV respectively. The results obtained from the reconstruction of D meson decays at central rapidity and from electrons from heavy-flavour hadron decay will be presented.

[hep-ex] 13 Aug 2013

arXiv:1308.2978v1

1 Introduction

The comparison of heavy-flavour hadron production in proton-proton and Pb–Pb collisions at the LHC offers the opportunity to investigate the properties of the high-density colour-deconfined state of strongly-interacting matter (Quark Gluon Plasma, QGP) that is expected to be formed in high-energy collisions of heavy nuclei. Due to their large mass, charm and beauty quarks are created in hard-scattering processes with high virtuality ($Q^2 \gtrsim 4m_{c[b]}^2$) involving partons of the incident nuclei, hence at the initial stage of the collision. They interact with the medium and lose energy via both inelastic (medium-induced gluon radiation, or radiative energy loss) [1, 2] and elastic (collisional energy loss) [3] processes. This in-medium energy loss, which is sensitive to the medium energy density, is expected to affect differently heavy quarks, gluons and light quarks. In QCD, quarks have a smaller colour coupling factor with respect to gluons, so that the energy loss for quarks is expected to be smaller than for gluons. In addition, the ‘dead-cone effect’ should reduce small-angle gluon radiation for heavy quarks with moderate energy-over-mass values [4]. A sensitive observable is the nuclear modification factor, defined, for a particle species h , as $R_{AA}^h(p_t) = \frac{dN_{AA}^h/dp_t}{\langle T_{AA} \rangle \times d\sigma_{pp}^h/dp_t}$, where N_{AA}^h is the yield measured in heavy-ion collisions, $\langle T_{AA} \rangle$ is the average nuclear overlap function calculated with the Glauber model [5] in the considered centrality range, and σ_{pp}^h is the production cross section in pp collisions. In-medium energy loss determines a suppression, $R_{AA} < 1$, of hadrons at moderate-to-high transverse momentum ($p_t \gtrsim 2$ GeV/c). By comparing the nuclear modification factors of pions (R_{AA}^π), mostly originating from gluon fragmentation, with that of hadrons with charm (R_{AA}^D) and beauty (R_{AA}^B) the dependence of the energy loss on the parton nature (quark/gluon) and mass can be investigated. A mass ordering pattern $R_{AA}^\pi(p_t) \lesssim R_{AA}^D(p_t) \lesssim R_{AA}^B(p_t)$ has been predicted [4, 6]. ALICE has studied open heavy-flavour production in pp and Pb–Pb collisions at mid-rapidity by measuring the p_t -differential production cross sections of electrons from heavy-flavour hadron decays [7, 8] and of D^0 , D^+ and D^{*+} mesons via exclusive reconstruction of hadronic decay channels [9, 10]. At forward rapidity, ALICE has measured the production of single muons coming from heavy-flavour hadron decays [11]. The large suppression observed in Pb–Pb collisions w.r.t. pp collisions, about a factor 3-4 for $p_t \gtrsim 5$ GeV/c, suggests that charm quarks strongly interact with the medium. It is natural then to wonder whether charm is thermalized.

In heavy-ion collisions with non-zero impact parameter the interaction region exhibits an azimuthal asymmetry with respect to the reaction plane (Ψ_{RP}), defined by the azimuth of the impact parameter and the beam direction.

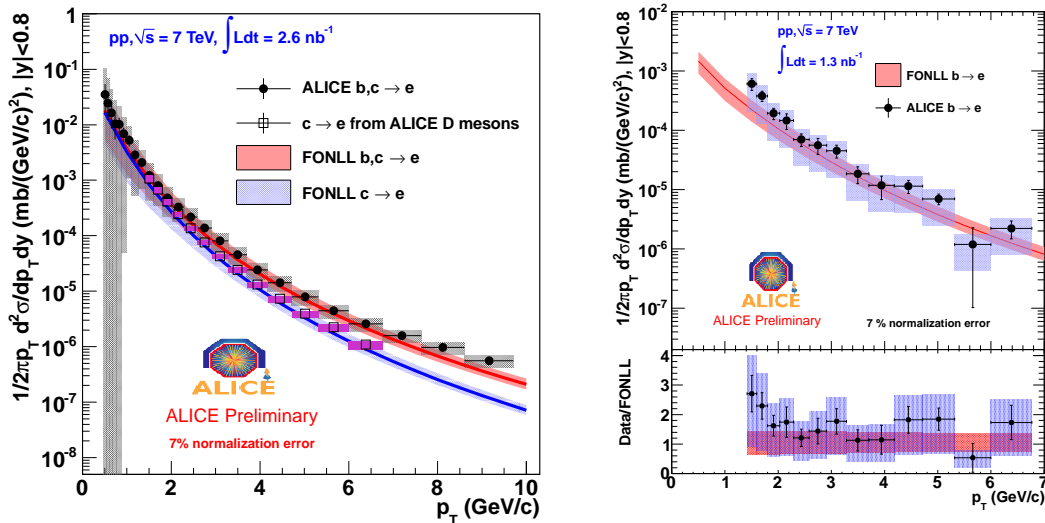


Figure 1: p_t -differential production cross section of electrons from the decay of hadrons carrying a charm or beauty quark (on the left), or a beauty quark (on the right) in pp collisions at $\sqrt{s} = 7$ TeV. The measurements are compared to FONLL predictions [23] (see text).

Collective effects convert this geometrical anisotropy into an asymmetry in momentum space that is reflected in the final hadron azimuthal distribution [12]. The effect, sensitive to the degree of thermalization of the system, can be evaluated by measuring the 2nd coefficient of the Fourier expansion of the azimuthal distribution, called elliptic flow (v_2) [12]. The measurement of the heavy-flavour particle v_2 can provide fundamental information on the degree of thermalization of charm quarks in the medium. Some models [13] predict charm elliptic flow to be smaller than that of light quarks at p_t up to ~ 2 GeV/ c and comparable at higher p_t . The PHENIX experiment at RHIC has measured the heavy-quark flow via non-photonic electrons, observing non-zero values ($v_2 \sim 0.09$ at $p_t \sim 1.5$ GeV/ c) [14]. ALICE has performed a preliminary measurement of the D^0 elliptic flow [15].

In these proceedings the measurements of the nuclear modification factor of electrons from heavy-flavour hadron decays R_{AA} and of D^0, D^+ and D^{*+} are reviewed as well as the preliminary measurement of the D^0 v_2 .

2 ALICE heavy-flavour probes at central rapidity

The ALICE detector, described in detail in [16], consists of a central barrel composed of various detectors for particle reconstruction at midrapidity, a forward muon spectrometer, and a set of forward detectors for triggering and event characterization. In particular, in the central pseudo-rapidity region ($|\eta| < 0.9$), tracks are reconstructed in the Time Projection Chamber (TPC) and in the Inner Tracking System (ITS), and then propagated out to the Transition Radiation Detector (TRD) and to the the Time Of Flight (TOF) detector. An Electromagnetic Calorimeter (EMCal) covers the pseudo-rapidity range $|\eta| < 0.7$ with an azimuthal acceptance of $\Delta\phi = 107^\circ$, limited to $\Delta\phi = 40^\circ$ in 2010 when the detector was not fully installed. The mentioned detectors are embedded in a 0.5 T magnetic field parallel to the LHC beam direction (z -axis in the ALICE reference frame). The VZERO detector, composed of two arrays of scintillator tiles covering the full azimuth in the pseudo-rapidity regions $2.8 < \eta < 5.1$ (VZERO-A) and $-3.7 < \eta < -1.7$ (VZERO-C), is used for triggering and for the determination of the event centrality, as described in detail in [17].

2.1 Electrons from heavy-flavour hadron decay

Electrons are identified at mid-rapidity ($|\eta| < 0.8$) using the information provided by the TPC, the TOF and the TRD. The EMCal is being included as well. The remaining hadron contamination is determined via fits of the TPC dE/dx in momentum slices and subtracted from the electron spectra. More details on the adopted electron identification criteria can be found in [7, 8]. In pp collisions, electrons are measured from $p_t = 0.5$ GeV/ c to

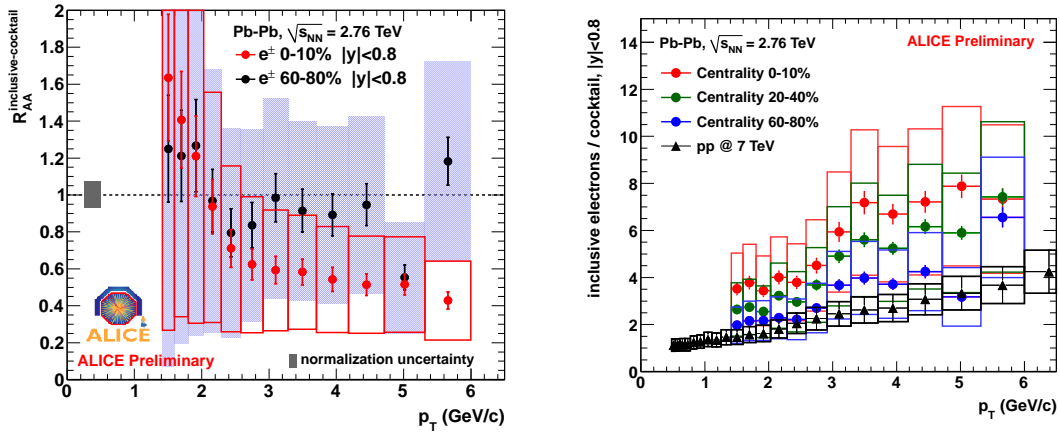


Figure 2: Left panel: R_{AA} of electrons from heavy-flavour hadron decay in central and peripheral Pb–Pb collisions at $\sqrt{s_{NN}} = 2.76$ TeV. Right panel: ratio between the inclusive electron spectrum and the spectrum of electrons not coming from heavy-flavour hadron decay, obtained with the cocktail technique (see text), in pp collisions and in Pb–Pb collisions at different centralities.

10 GeV/ c . The hadron contamination amounts to less than 5%. In Pb–Pb collisions, electrons are measured from 1.5 GeV/ c to 6 GeV/ c . The TRD has not been included yet in the analysis. The hadron contamination is therefore larger than in the pp case and reaches about 10% at 6 GeV/ c .

The inclusive electron yield is corrected for acceptance, tracking and particle identification efficiency using Monte Carlo simulation. In addition to electrons from heavy-flavour hadron decays, that constitute the main contribution at high p_t ($p_t \gtrsim 2$ GeV/ c in pp collisions), the inclusive spectrum contains background electrons from Dalitz decay of light mesons (mainly π^0), from the conversion in the material of photons from π^0 decay, Dalitz decays and direct radiation, and from dielectron decays of vector mesons (mainly from ρ, ω, ϕ , at low p_t , also from heavy quarkonia at high p_t). Photon conversion and π^0 Dalitz decay represent the largest background contribution. To reduce the latter contribution the tracks used in the analysis are required to have a hit in the innermost pixel layer, positioned at a radius of 3.9 cm from the beam line. In order to obtain the spectrum of electrons from heavy-flavour hadron decay, a MC event generator is used to calculate a “cocktail” of background electrons, starting from the pion spectrum measured with ALICE and relying on m_t -scaling for the heavier mesons [7].

2.2 Reconstruction of D meson hadronic decays with the ALICE detector

ALICE has measured the production of D^0 , D^+ ($c\tau \approx 123$ and $312 \mu\text{m}$ respectively [18]) and D^{*+} (strong decay) in pp and Pb–Pb collisions at central rapidity ($|y| < 0.5$) via the exclusive reconstruction of the decays $D^0 \rightarrow K^- \pi^+$ (with branching ratio, $\text{BR} = 3.89 \pm 0.05\%$ [18]) and $D^+ \rightarrow K^- \pi^+ \pi^+$ ($\text{BR} = 9.4 \pm 0.4\%$ [18]) and $D^{*+} \rightarrow D^0 \pi^+$ ($\text{BR} = 67.7 \pm 0.5\%$ [18]). The analysis strategy for the extraction of the signals out of the large combinatorial background from uncorrelated tracks is based on the reconstruction and selection of secondary vertex topologies with significant separation (typically a few hundred micrometer) from the primary vertex [9]. The TPC and the ITS detectors provide a spatial resolution on the track position in the vicinity of the primary vertex of the order of few tens of microns at sufficiently high p_t [19]. Tracks with $|\eta| < 0.8$ and displaced from the primary vertex are selected to reconstruct D^0 and D^+ meson candidates. D^{*+} candidates are obtained by combining the D^0 candidates with tracks with transverse momentum $p_t > 0.08$ GeV/ c in pp collisions and, in Pb–Pb collisions, $p_t > 0.2$ GeV/ c in the centrality range 0–20% and $p_t > 0.1$ GeV/ c in 20–80%. Good alignment between the reconstructed meson momentum and the flight direction between the primary and secondary vertex is also required. The identification of the charged kaon in the TPC and TOF detectors provides additional background rejection. A particle identification strategy that preserves most of the D meson signal was adopted. Similar analyses were performed on pp and Pb–Pb data, with a tighter selection in the latter case, dictated by the higher combinatorial background. To extract the signal, in the D^0 and D^+ cases a fit to the invariant mass distribution is performed, while, for D^{*+} mesons, the mass difference $\Delta m = m_{D^{*+}} - m_{D^0}$ distribution is fitted. The ‘raw’ signal is corrected

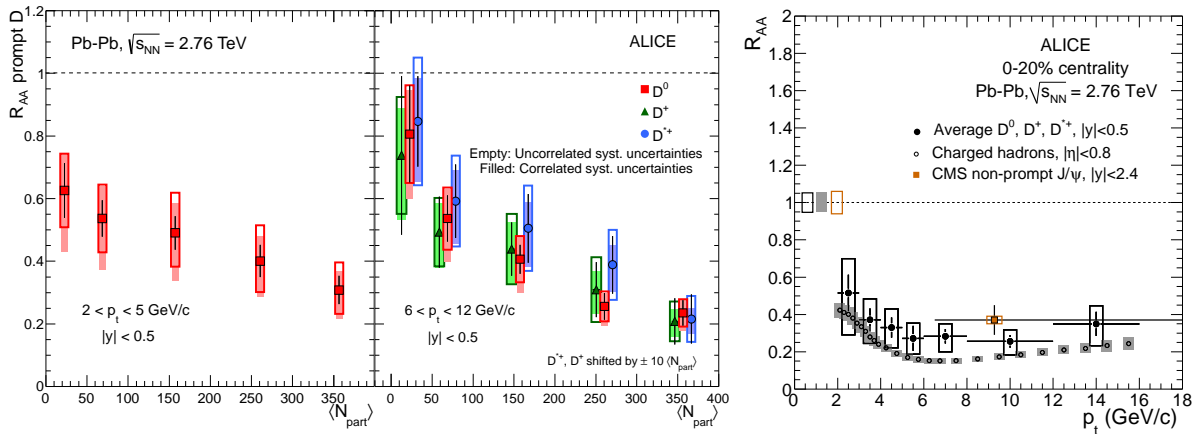


Figure 3: Left panel: D^0 , D^+ and D^{*+} nuclear modification factor measured in central (0 – 20%) Pb–Pb collisions as a function of centrality for $2 < p_t < 5$ GeV/c (left) and $6 < p_t < 12$ GeV/c (right). The filled boxes represent the systematics uncertainties correlated among the different centrality intervals. Right panel: Average D^0 , D^+ and D^{*+} nuclear modification factor as a function of p_t measured in central (0 – 20%) Pb–Pb collisions, compared to the R_{AA} of charged hadrons [29] and of non-prompt J/ψ from B decay [30]. The boxes around $R_{AA} = 1$ represent the uncertainty on the normalization of the pp reference and on $\langle T_{AA} \rangle$. Both plots are taken from [10].

for acceptance and efficiency using Monte Carlo simulations based on Pythia (Perugia-0 tuning) [20, 21] and HIJING [22] event generators. The contribution of D mesons from B decays was evaluated relying on the FONLL prediction [23], which describes well bottom production at the Tevatron [24] and at the LHC [25, 26]. The systematic error due to the FONLL theoretical uncertainty on beauty prediction was estimated from the spread of the results recovered using the minimum and maximum predictions for secondary D meson production. In the Pb–Pb case, the FONLL prediction of secondary D meson production in pp collisions is multiplied by $\langle N_{\text{coll}} \rangle \times R_{AA}^B$, where the hypothesis on the B meson R_{AA} encodes all potential nuclear and medium effects affecting B production.

3 Results from proton-proton collisions at $\sqrt{s} = 7$ TeV

Figure 1 shows on the left the p_t differential cross section of electrons from heavy-flavour hadron decay (black circles), as measured on a minimum-bias sample of pp collisions at $\sqrt{s} = 7$ TeV corresponding to an integrated luminosity of $L_{\text{int}} = 2.6 \text{ nb}^{-1}$. The systematic uncertainty is about 20% on the inclusive electron spectrum, dominated by the electron identification uncertainty, and about 10% on the cocktail. At low p_t electrons from charm hadron constitute the main contribution, as clearly visible from the comparison with the cross section of electron from D meson decay, deduced from the D meson p_t -differential cross sections [9] by applying PYTHIA decay kinematics and displayed in the same panel (pink square markers). Electrons from b hadron decay can be selected by requiring that the electron track is displaced with respect to the primary vertex of the collision. The measured cross section, based on the analysis of a sub-sample with $L_{\text{int}} = 1.3 \text{ nb}^{-1}$ and reported on the right panel of Fig. 1, is compatible with that obtained by subtracting the electron-from-D cross section from the heavy-flavour electron cross section. The measurements are well reproduced, within uncertainties, by FONLL predictions [23], based on perturbative QCD calculations.

As reported in [9], ALICE has measured the p_t -differential production cross sections in pp collisions at $\sqrt{s} = 7$ TeV in the momentum range $1 < p_t < 16$ GeV/c for D^0 and in the range $1 < p_t < 24$ GeV/c for D^{*+} and D^+ . The measurements, based on the analysis of a minimum-bias sample with $L_{\text{int}} = 5 \text{ nb}^{-1}$, are well described by predictions based on pQCD calculations as FONLL [23] and GM-VFNS [27].

To provide the reference cross section at 2.76 TeV, needed to compute the R_{AA} , the measurements at 7 TeV are scaled by the ratio of FONLL predictions at $\sqrt{s} = 2.76$ and 7 TeV [28]. In March 2011 a sample of $\approx 6.5 \times 10^7$ events from pp collisions at $\sqrt{s} = 2.76$ TeV was collected. The D^0 and D^+ signals were measured in the range $2 < p_t < 8$ GeV/c. For D mesons, while the accumulated statistics did not allow for determining a pp reference over the whole momentum range, it provided an important cross check of the theoretical scaling procedure in the

momentum range where the data sets overlap. A similar measurement is being carried out for the electron decay channel and, in this case, should provide a reduction of the systematic uncertainty on the pp reference.

4 Results from Pb–Pb collisions at $\sqrt{s_{\text{NN}}} = 2.76$ TeV

The data from Pb–Pb collisions at centre-of-mass energy $\sqrt{s_{\text{NN}}} = 2.76$ TeV were collected with an interaction trigger based on the information of the SPD and the VZERO detector. In total, 13×10^6 Pb–Pb events with centrality in the range 0–80% were used in the analyses. The corresponding integrated luminosity is $L_{\text{int}} = 2.12 \pm 0.07 \mu\text{b}^{-1}$.

4.1 Heavy-flavour electron nuclear modification factor

Figure 2 shows on the left-hand panel the R_{AA} of cocktail-subtracted electrons in central (0 – 10%) and peripheral (60 – 80%) Pb–Pb collisions. In peripheral collisions, R_{AA} is compatible with one. In central collisions, a suppression is observed in the range $3.5 < p_{\text{t}} < 6$ GeV/ c that, due to the large uncertainties, can be estimated in a factor between 1.2 and 5. On the right-hand panel, the ratio between the inclusive electron spectrum and the background cocktail is reported for different centralities and for pp collisions. In pp collisions, the ratio approaches unity towards low p_{t} , where the inclusive electron spectrum is dominated by electrons from background sources. In Pb–Pb collisions, this ratio is larger, especially in the most central collisions, causing the R_{AA} rise towards low p_{t} . The effect, still under investigation, suggests the presence of a further source of electrons: a possible candidate is thermal radiation, observed by the PHENIX experiment below 3 GeV/ c in Au–Au collisions at RHIC [31].

4.2 D meson nuclear modification factors

The D meson production is suppressed by a factor 4–5 in central (0 – 10%) events for $p_{\text{t}} \gtrsim 6$ GeV/ c , as quantified by the nuclear modification factors shown in Fig. 3 as a function of the centrality, expressed in terms of the average number of participant nucleons, $\langle N_{\text{part}} \rangle$, at low (left, D^0 only) and high p_{t} (middle). At high p_{t} , R_{AA} decreases from ≈ 0.81 in peripheral ($\langle N_{\text{part}} \rangle = 23$) to ~ 0.2 in central ($\langle N_{\text{part}} \rangle = 357$) events. The D^0, D^+ and D^{*+} R_{AA} agree within errors. Their average, calculated using the statistical uncertainty as weight and taking into account the correlation among the systematic uncertainties of the different channels, is shown on the right-hand panel of Fig. 3 as a function of p_{t} . In the same panel the R_{AA} of charged hadrons [29] and that, measured by CMS, of non-prompt J/ψ from b-hadron decay [30] are displayed. In central collisions, R_{AA} decreases with p_{t} from ~ 0.51 at low p_{t} to ≈ 0.27 at high p_{t} . The average R_{AA} is very close to the D^0 R_{AA} , measured with a smaller statistical uncertainty (15 – 20%) than for D^+ and D^{*+} . The estimated total systematic uncertainty, accounting for the uncertainties on the signal extraction procedure, on track reconstruction efficiency, on the MC corrections for reconstruction acceptance, cut and PID selection, is of the order of 30 % at intermediate p_{t} , $^{+35\%}_{-45\%}$ for $2 < p_{\text{t}} < 3$ GeV/ c and $^{+32\%}_{-40\%}$ for $12 < p_{\text{t}} < 16$ GeV/ c . The hypothesis on R_{AA}^{B} , which is done to subtract the feed-down from B mesons as explained in section 2.2, is varied in order to span the range $1/3 < R_{\text{AA}}^{\text{D}}/R_{\text{AA}}^{\text{B}} < 3$, with $R_{\text{AA}}^{\text{D}}/R_{\text{AA}}^{\text{B}}$ calculated a posteriori. The range of R_{AA}^{D} values obtained in each p_{t} bin is considered as the systematic error due to the R_{AA}^{B} assumption. For the D^0 , the maximum spread is $^{+14\%}_{-27\%}$ in the bin $12 < p_{\text{t}} < 16$ GeV/ c .

The D meson R_{AA} is compatible, within errors, with the R_{AA} of charged hadrons and of non-prompt J/ψ from b-hadron decay. However, considering that the systematic uncertainties of D mesons are not fully correlated with p_{t} there is an indication for $R_{\text{AA}}^{\text{D}} > R_{\text{AA}}^{\text{charged hadrons}}$. More precise and more p_{t} -differential measurements of the non-prompt J/ψ R_{AA} are necessary to conclude on the possible difference between charm and beauty suppression. In addition to final state effects, where parton energy loss would be predominant, also initial-state effects are expected to influence the measured R_{AA} . In the kinematic range relevant for charm production at LHC energies, the main expected effect is nuclear shadowing, which reduces the parton distribution functions for partons with nucleon momentum fraction x below 10^{-2} . The effect of shadowing on the D meson R_{AA} was estimated using the MNR next-to-leading order (NLO) perturbative QCD calculation [34] and the nuclear modification of the parton distribution functions from the EPS09 parametrization [35]. As shown in Fig. 4 (left-hand panel) nuclear shadowing yields a relatively small effect for $p_{\text{t}} \gtrsim 5$ GeV/ c ($0.85 < R_{\text{AA}}^{\text{D}} < 1.08$ at $p_{\text{t}} = 5$ GeV/ c). Therefore, the observed suppression can be considered as an evidence of in-medium charm quark energy loss.

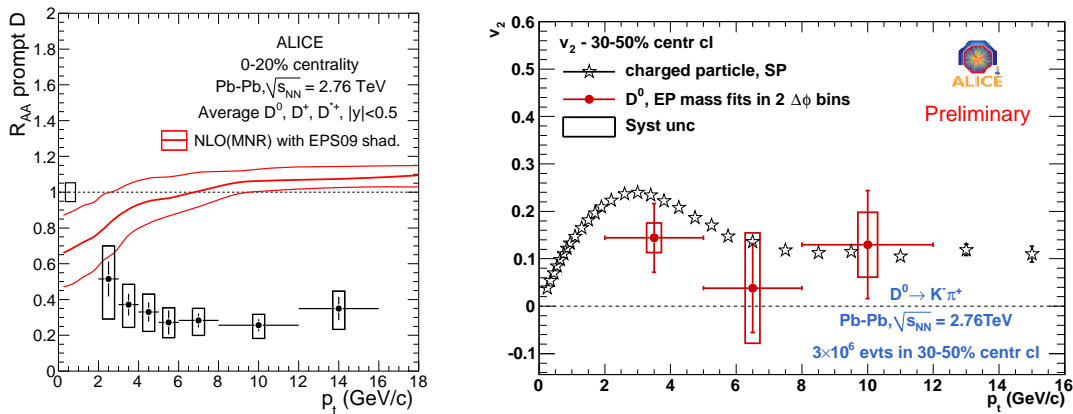


Figure 4: Left (from [10]): Average R_{AA} of D mesons in the 0–20% centrality class compared to the expectation from NLO pQCD [34] with nuclear shadowing [35]. Right: D^0 v_2 as a function of p_t , obtained with the 2 $\Delta\phi$ method (see text). The vertical lines represent the statistical errors while the boxes the systematic uncertainties.

5 D^0 meson elliptic flow

The first D^0 v_2 measurement [15] was performed with event plane methods and 2-particle cumulants [32]. In the event plane methods, the correlation of D^0 azimuthal angle (ϕ) to the reaction plane Ψ_{RP} is analyzed. The reaction plane is estimated via the event plane Ψ_2 , by the so-called Q_2 -vector, which is obtained from a weighted sum of the azimuthal angles of all TPC tracks with $|\eta| < 0.8$, satisfying quality requirements. Three different techniques were used to measure an “observed” v_2^{obs} which is then corrected by the event-plane resolution, estimated from sub-events, to measure v_2 . In the first method, an in-plane and an out-of-plane region of $\Delta\phi = \phi - \Psi_2$ are defined and the signals N_{IN} and N_{OUT} are extracted by fitting the invariant mass distributions observed in the two regions. The v_2^{obs} is recovered as

$$v_2^{obs} = \frac{\pi N_{IN} - N_{OUT}}{4 N_{IN} + N_{OUT}}. \quad (1)$$

In the second approach v_2^{obs} is estimated as the average of the $\cos(2\Delta\phi)$ distribution observed in the invariant mass D^0 signal region after the subtraction of the background distribution obtained from the side bands. In the third method, the distribution of $v_2^{obs}(M) = \langle \cos(2\Delta\phi) \rangle(M)$ is fitted with a two component function, which includes a background term $v_2^{obs\ back}(M)$ and a signal term $v_2^{obs\ sign}$, weighted by the background and signal fractions, which are estimated as a function of the invariant mass, from the invariant mass fit. A linear function is used for the $v_2^{obs\ back}(M)$ component. The v_2 measurement with the 2 $\Delta\phi$ technique is reported, for the centrality range 30 – 50%, on the right-hand panel of Fig. 4 as a function of p_t and compared to the charged hadron v_2 . The precision of the measurement is still limited by the available statistics (3×10^6 events): within 1.8σ a non-zero v_2 is measured for D^0 mesons in the range $2 < p_t < 5$ GeV/ c . Within errors, compatible results are obtained with the techniques described above and with the cumulant approach (see [15] for more details). The analysis of Pb–Pb data collected in 2011 will clarify whether charm v_2 is really non-zero and how it does compare to lighter hadron elliptic flow.

6 Summary

ALICE has measured charm and beauty production in pp collisions at 7 TeV and Pb–Pb collisions at $\sqrt{s_{NN}} = 2.76$ TeV via the reconstruction of D meson hadronic decays and single electron from heavy flavour hadron decays. Calculations based on perturbative QCD, like FONLL [23] and GM-VFNS [27], reproduce the p_t -differential cross section measured in pp collisions within the uncertainties. In Pb–Pb collisions the observed suppression of the production of D mesons as well as of cocktail-subtracted electrons for $p_t > 3.5$ GeV/ c indicates strong coupling of heavy quarks to the medium created in central heavy-ion collisions. The large uncertainties on the measurement

of D^0 elliptic flow does not allow to conclude whether charm is thermalized or not: the Pb–Pb data collected in 2011 should provide the required statistics to answer to this question.

References

- [1] M. Gyulassy and M. Plumer, Phys. Lett. **B243** (1990) 432.
- [2] R. Baier, Y. L. Dokshitzer, A. H. Mueller, S. Peigne and D. Schiff, Nucl. Phys. **B484** (1997) 265.
- [3] M. H. Thoma and M. Gyulassy, Nucl. Phys. **B351** (1991) 491.
E. Braaten and M. H. Thoma, Phys. Rev. **D44** (1991) 1298; Phys. Rev. **D44** (1991) 2625.
- [4] Y. L. Dokshitzer, D. E. Kharzeev, Phys. Lett. **B519** (2001) 199.
N. Armesto, C. A. Salgado and U. A. Wiedemann, Phys. Rev. **D69** (2004) 114003.
M. Djordjevic, M. Gyulassy, Nucl. Phys. **A733** (2004) 265.
B.-W. Zhang, E. Wang and X.-N. Wang, Phys. Rev. Lett. **93** (2004) 072301.
S. Wicks, W. Horowitz, M. Djordjevic and M. Gyulassy, Nucl. Phys. **A783** (2007) 493.
- [5] R. J. Glauber in Lectures in Theoretical Physics, NY, 1959, Vol. 1, 315.
M. Miller *et al.*, Ann. Rev. Nucl. Part. Sci. **57** (2007) 205.
- [6] N. Armesto, A. Dainese, C.A. Salgado and U.A. Wiedemann, Phys. Rev. **D71** (2005) 054027.
- [7] S. Masciocchi for the ALICE Coll., J. Phys. **G38** (2011) 124069.
- [8] R. Bailhache for the ALICE Coll., Acta Physica Polonica B *Proceedings supplement* Vol. 5, No. 2 (2012) 291.
- [9] B. Abelev *et al.* [ALICE Coll.], JHEP **01** (2012) 128.
- [10] B. Abelev *et al.* [ALICE Coll.] arXiv:1203.2160v1, submitted to JHEP.
- [11] L. Manceau for the ALICE Coll., these proceedings.
- [12] N. Armesto *et al.*, J. Phys. **G35**, (2008) 054001.
- [13] D. Molnar, J. Phys. **G31**, (2005) S421-S428.
- [14] A. Adare *et al.* [PHENIX Coll.], Phys. Rev. Lett. **98**, (2007) 172301.
- [15] C. Bianchin for the ALICE Coll., Acta Physica Polonica B *Proceedings supplement* Vol. 5, No. 2 (2012) 335.
- [16] K. Aamodt *et al.* [ALICE Coll.], JINST **3** (2008) S08002.
- [17] A. Toia for the ALICE Coll., J. Phys. **G38** (2011) 124007.
- [18] K. Nakamura *et al.* (Particle Data Group), J. Phys. **G37**, (2010) 075021.
- [19] A. Rossi *et al.* [ALICE Coll.], PoS(Vertex2010)017, arXiv:1101.3491.
- [20] T. Sjöstrand, S. Mrenna, P. Skands, JHEP **05** (2006) 026.
- [21] P. Z. Skands, arXiv:0905.3418 [hep-ph] (2009).
- [22] X.-N. Wang and M. Gyulassy, Phys. Rev. **D 44** (1991) 3501.
- [23] M. Cacciari, M. Greco, P. Nason, JHEP **9805** (1998) 007.
M. Cacciari, S. Frixione and P. Nason, JHEP **0103** (2001) 006.
- [24] M. Cacciari *et al.*, JHEP **0407** (2004) 033; private communication.
- [25] R. Aaij *et al.* [LHCb Coll.], Phys. Lett. **B694** (2010) 209-216.
- [26] V. Khachatryan *et al.* [CMS Coll.], arXiv:1011.4193.
- [27] B.A. Kniehl *et al.*, Phys. Rev. Lett. **96** (2006) 012001.
B.A. Kniehl, G. Kramer, I. Schienbein, and H. Spiesberger, in preparation.
- [28] R. Averbek, N. Bastid, Z. Conesa del Valle, A. Dainese, X. Zhang, arXiv:1107.3243 (2011).
- [29] ALICE Collaboration, Centrality dependence of charged-hadron transverse momentum distributions in Pb–Pb collisions at $\sqrt{s_{NN}} = 2.76$ TeV, article in preparation.
- [30] CMS Collaboration, arXiv:1201.5069 [nucl-ex] (2012).
- [31] A. Adare *et al.* [PHENIX Coll.], Phys. Rev. Lett. **104**, (2010) 132301.
- [32] N. Borghini, P. M. Dinh, J. Y. Ollitrault, Phys. Rev. **C64** (2001) 054901.
- [33] A. Bilandzic, R. Snellings, and S. Voloshin, Phys. Rev. **C83** (2001) 044913.
- [34] M. Mangano, P. Nason and G. Ridolfi, Nucl. Phys. **B373** (1992) 295.
- [35] K. J. Eskola, H. Paukkunen and C. A. Salgado, JHEP **04** (2009) 065.